Offset vector tile gather extension and weighting to reduce footprint in dual-datum and converted-wave migration

Vetle Vinje, Peng Zhao and James Gaiser, CGG*

Summary

Common-offset vector (COV) binning provides single-fold data sets that can be migrated with surface offset and azimuth preserved. The latter allows post-migration processing such as Radon demultiple or azimuthal residual moveout flattening to enhance the quality of the final stacked image. Single fold coverage enables each COV volume to produce a clean image with limited migration-operator artefacts, and with the potential to preserve the AVO character. However, in the COV domain, this works only for surveys with sources and receivers on the same acquisition datum and with a single-mode arrival having symmetric ray paths in a flat earth (such as P-waves). Irregular subsurface illumination for dual-datum acquisition or mode-converted PS-wave data causes artefacts in migration of COV binned data, including acquisition footprints. Here we describe a technique to reduce these artefacts. The method bins recorded data into gathers corresponding to each offset vector tile (OVT) and computes time and velocity-model dependent weighting and muting functions for each OVT gather in such a way that uniform illumination is obtained at all levels beneath a reference level.

Introduction

The concept of common-offset vector binning was introduced almost simultaneously by Vermeer (1998 and 2002) and Cary (1999) as an alternative to cross-spread binning for 3D wide-azimuth surveys. Conventional cross-spread processing assumes that reflection points and common mid-points (CMPs) share the same lateral location. However, ocean-bottom data and mode-converted PS-waves violate this assumption. Recently, Stewart and Gaiser (2011), Bale et al. (2013) and Gaiser (2014) have revisited COV processing problems of PS-waves, and demonstrated corrections for illumination area distortion.

In this paper we address problems with COV illumination for PP- and PS-waves of various geometries. The aim is to improve the reflection point distribution within a COV image. As opposed to Stewart and Gaiser (2011) and Bale et al. (2013) we describe *time-dependent* corrections of offset-vector tile gathers that can be applied for orthogonal cross-spread PS-wave land data and for PP- or PS-wave marine data of dual-datum ocean-bottom geometries.

COV binning and distortions of reflection points

An OVT from a cross-spread ocean-bottom acquisition is shown in Figure 1a. The key parameters are shown in Table 1.

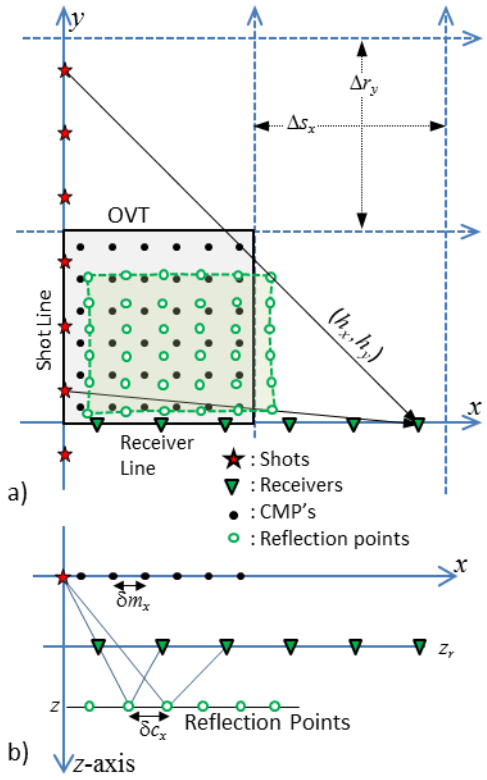

Figure 1: Cross-spread acquisition with sources, receivers and reflection points associated with a near-offset OVT and an OVT gather shown in top-view a), and side view b).

Shots are located in lines parallel to the *y*-axis at the surface while receivers are located on the water bottom on lines parallel to the *x*-axis. The black square is the OVT and the stars and triangles are the associated shots and receivers, respectively. These shots/receiver pairs create a subset of the recorded data that we call the ***OVT gather***.

The size of this gather in offset vector space is $(\Delta H_x, \Delta H_y) = (2\Delta s_x, 2\Delta r_y)$.

DOI http://dx.doi.org/10.1190/segam2015-5899618.1

Distance between shot lines:		Δs_x
Distance between receiver lines:		Δr_y
Increment of shots along shot lines:		δs_y
Increment of receivers along receiver lines:		δr_x
Offset vector from shot to receiver:	$\mathbf{h}$ =	(h_x, h_y)
Center offset vector of the OVT:		(hm_x, hm_y)
Tile size:		$(\Delta s_x, \Delta r_y)$
Bin size:		$(\delta r_x/2, \delta s_y/2)$
Standard OVT gather size:	$(\Delta H_x, \Delta H_y)$ =	$(2\Delta s_x, 2\Delta r_y)$
CMP increment:		$(\delta m_x, \delta m_y)$
Reflection point increment:		$(\delta c_x, \delta c_y)$

Table 1: Key quantities in the cross spread acquisition in Figure 1

For P-waves with sources and receivers on the same datum the standard OVT gather size (ΔH_x, ΔH_y) will give a single fold data set with even illumination of subsurface flat reflectors. However, for dual-datum acquisition, and/or for PS-waves, the reflection point and the CMP will not coincide.

Figure 1b shows the *xz* view of the cross-spread acquisition with a source (red star) at the surface, the receivers (green triangles) at the water bottom at depth z_r and the rays reflected from an interface at depth *z*. Due to the asymmetry of the ray paths the reflection point increment δc_x is larger than the CMP increment δm_x. Reflection points will be pushed towards the receiver, creating an extended and shifted illuminated area in the x-direction. In the y-direction δc_y is less than δm_y and again reflection points are shifted towards the receiver, shrinking and shifting the illuminated area in this direction. The result is a reflection point area for this OVT shown as the dotted green rectangle in Figure 1a, where the green circles indicate the reflection points. This creates subsurface overlaps and non-illuminated zones when adjacent OVTs are migrated, and is a significant cause of imaging distortions and footprints. This distortion depends on the depth of the reflector. For a shallow reflector the distortion is large. As the depth of the reflector increases, the illuminated area of the reflector asymptotically approaches the standard tile size of (Δs_x, Δr_y).

Method

The illumination distortions described above can be corrected by adjustments of the size of the OVT gather. In order to improve the illumination for a range of depth levels in the model this adjustment is time-dependent.
Figures 2 and 3 illustrate this principle on the cross-spread acquisition of Figure 1.

In Figure 2, a *yz* projection of a shot line and three cross-spread receiver lines are shown. The receivers are located at the water bottom at depth z_r beneath the shot level.

Due to the different datums of sources and receivers, the standard OVT gather size of ΔH_y is not sufficient to create complete illumination of the reflector at depth *z*. The width of the illuminated area is less than the tile width Δr_y. There will also be illumination distortions in the *xz* projection, but in this case the illuminated area will be larger than the tile size Δs_x.

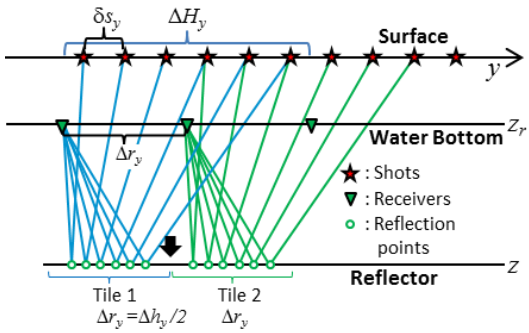

Figure 2: Projection of a shot line and three receiver lines in Figure 1 into the *yz* plane. The standard OVT gather size of ΔH_y creates illumination holes at the reflector (black arrow).

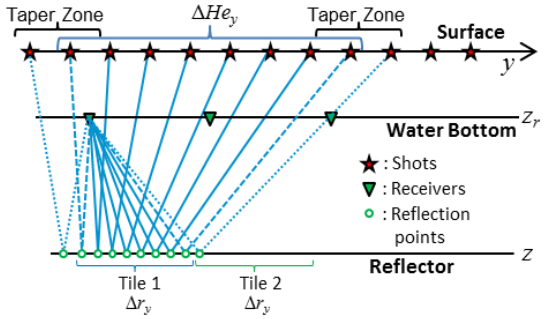

Figure 3: The OVT gather size in the *y*-direction is increased to ΔHe_y to ensure full illumination of the tile at the reflector level.

In order to create a complete illumination of the reflectors, the standard shot group size ΔH_y (Figure 2) is extended to ΔHe_y (Figure 3), plus a taper zone, adding more traces into the OVT gather.

The additional length in ΔHe_y is a function of the depth of the reflector. In order to reduce the footprint effect further, the traces at the edges of the OVT gather are tapered with a $\cos^2$ taper. Also in the *x*-direction the standard OVT gather size is adjusted, but due to the geometry (as shown in Figure 1b) ΔHe_x is smaller than ΔH_x, such that fewer traces are included in the gather.

DOI http://dx.doi.org/10.1190/segam2015-5899618.1

So how can we find a depth- and time-dependent OVT gather size (ΔHe_x, ΔHe_y) that creates uniform illumination in all depth levels of the subsurface? We start by defining ratios R_x and R_y between the reflection point density and the CMP density

$$R_x = \frac{dc_x}{dm_x} \quad \text{and} \quad R_y = \frac{dc_y}{dm_y}, \qquad (1)$$

where $R_x(z,\mathbf{h})$ and $R_y(z,\mathbf{h})$ are functions of depth z and offset vector $\mathbf{h}=(h_x, h_y)$. In the practical computation of R_x and R_y we assume a local 1D model in each tile center (x,y)-position, as described below. The extension factors ΔHe_x and ΔHe_y are given by the solution to the integrals

$$\int_{hm_x-\frac{\Delta He_x}{2}}^{hm_x+\frac{\Delta He_x}{2}} R_x(z,h_x,h_y)\,dh_x = \Delta H_x \quad \text{and}$$

$$\int_{hm_y-\frac{\Delta He_y}{2}}^{hm_y+\frac{\Delta He_y}{2}} R_y(z,h_x,h_y)\,dh_y = \Delta H_y \qquad (2)$$

As can be seen from equation (2), $\Delta He_x = \Delta He_x(z,hm_x,h_y)$ and $\Delta He_y = \Delta He_y(z,hm_y,h_x)$. For the special case when $\delta c=\delta m$ we have symmetrical ray paths and $R_x=R_y=1$, giving $\Delta He_x=\Delta H_x$ and $\Delta He_y=\Delta H_y$. Thus, for symmetrical ray paths, there is no need to extend (or shrink) the size of the OVT gather relative to the standard OVT gather size.

In the practical implementation of OVT gather extension and weighting we compute R_x and R_y in equation (1) using ray tracing in local 1D velocity models. The 1D model is extracted from the vertical column of the 3D migration model in the spatial (x,y) center of each OVT. As an alternative, analytical approximations in 1D models can also be implemented (Gaiser, 2014). These approximations are a function of the velocity ratios of downgoing to upgoing rays (V_P/V_S in the case of PS-waves).

We also use ray tracing in the 1D model to find the mapping from time to depth, $z(t,\mathbf{h})$. The functions $\Delta He_x(z,hm_x,h_y)$, $\Delta He_y(z,hm_y,h_x)$, $R_x(z,\mathbf{h})$, $R_y(z,\mathbf{h})$ and $z(t,\mathbf{h})$ are then used to generate the extended OVT gather shown in Figure 4a which shows a 3D sketch of an OVT gather with x offset (h_x) and y offset (h_y) along the horizontal axes.

The blue rectangle shows the standard OVT gather size, ΔH_x and ΔH_y,, which remains constant for all times, t. The dotted red rectangles show the time-dependent outline of the non-muted part of the OVT gather as required to produce uniform illumination at variable depths. The outline is given by the time-dependent ΔHe_x and ΔHe_y centered on the central offset hm_x, hm_y.

Figure 4b shows a $[h_y,t]$ cross-section (i.e., constant h_x) through an OVT gather with the standard OVT gather size ΔH_y shown with dotted white lines and the depth/time dependent ΔHe_y in orange. The depth dependency is achieved by muting outside the orange ΔHe_y lines.

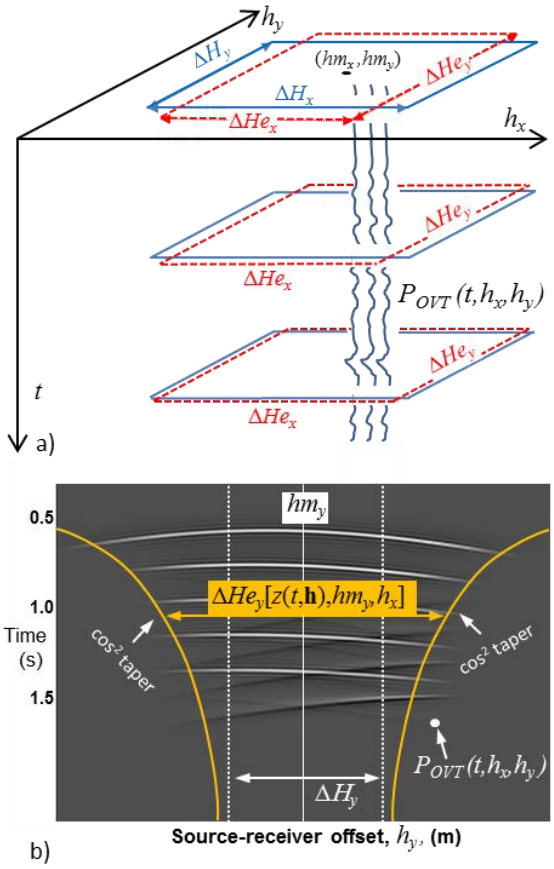

Figure 4: The OVT gather is a collection of pre-migration traces associated to a specific tile. The wiggles in a) indicate 3 of the traces in the OVT gather. b) shows a $[h_y,t]$ cross-section through the OVT gather in a).

A trace sample $P_{OVT}(t,h_x,h_y)$ indicated by a white dot and arrow in Figure 4b will be muted if $|h_y-hm_y| > \Delta He_y[z(t,\mathbf{h}),hm_y,h_x]/2$. The boundary between muted and non-muted parts of the OVT gather is tapered with a $\cos^2$ taper which will ensure a summation to unity in the image when all the OVT gathers for an offset class are migrated, and thus reduce footprints further.

In addition to the muting and tapering of the OVT gather we also need to correct for the distortions in the illumination density of the subsurface. For this, each trace

DOI http://dx.doi.org/10.1190/segam2015-5899618.1

is scaled with the factor $[R_x(z,\mathbf{h})R_y(z,\mathbf{h})]^{-1}$. In the special case of symmetrical ray paths R_x=R_y=1 the scaling factor is 1, as expected.

dependent, can be computed analytically or by ray tracing, and assume that the 3D model is locally 1D. The field-data example demonstrates significant improvement in imaging the shallow and intermediate subsurface using this method.

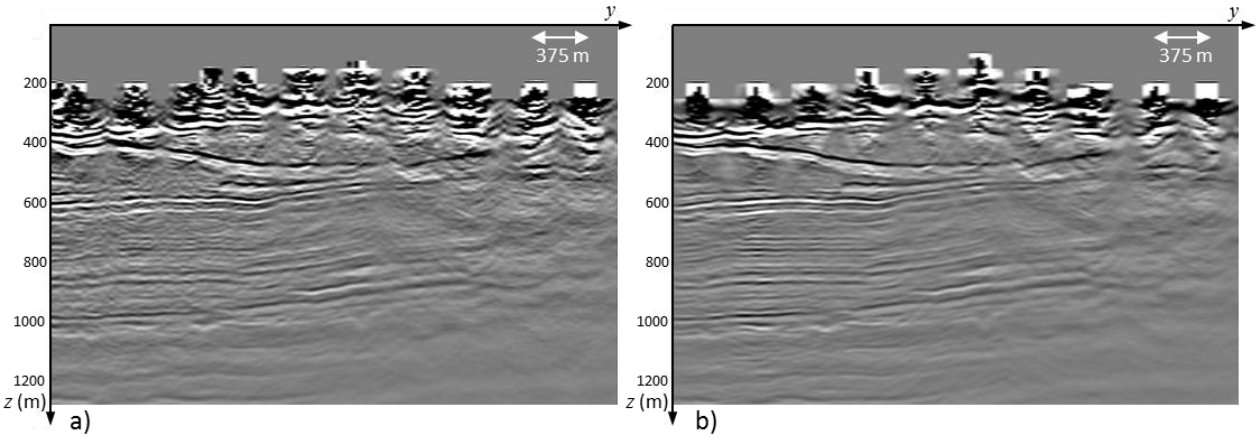

Figure 5: Kirchhoff migrated stacked sections based on a) conventional COV binning and b) the OVT gather weighting. Continuity is improved along the reflectors and migration noise is reduced.

Results

The field data example is from the Caspian Sea using ocean bottom cables oriented east-west with a separation of 375 m. The water depth in the area varies between 200 and 300 m which will create illumination distortions in imaging. A dense carpet, 50 m by 50 m, of air gun sources was fired near the water surface. This acquisition gives COV classes of 100 x 750 m offset size. The OVT extension/muting technique described above was applied on this data set to generate the extended COV classes suitable for migration.

The illumination correction of the OVT gathers was applied from z = 400 m and downwards. A total of 31 x 3 COV classes were migrated and then stacked after angle mute at 30 degrees. Figure 5 shows a crossline through the stacked volumes from (a) the conventional COV binning and (b) the OVT extension and muting technique. The imprint of the receiver cables are visible on both images in the very shallow, but both footprint and migration noise is greatly reduced in the intermediate and deeper parts of the image using OVT extension and muting.

Conclusions

Imaging converted wave and deep-water ocean-bottom data produces migration artifacts from uneven illumination achieved with regular acquisition geometries. In this paper we demonstrated a method to reduce these artefacts by a time-dependent extension and weighting of the OVT gathers. The transformation functions are velocity-model

Acknowledgements

We would like to thank Carl-Inge Nilsen from CGG Research for processing the OVT muted gathers, Naphtali Latter in CGG Subsurface Imaging (SI) for the conventional COV processing and Julian Holden and Ross Haacke, CGG SI for useful input and discussions. In addition, we would like to thank CGG for letting us publish this paper and SOCAR (the State Oil Company of the Azerbaijan Republic), BP Exploration (Caspian Sea) Limited ('BPXCS') and BPXCS's co-venturers in Azerbaijan International Operating Company (Chevron, Inpex, Statoil, Exxon Azerbaijan Limited, TPAO, Itochu and ONGC Videsh Ltd.) for allowing us to show the real example as part of the paper.

DOI http://dx.doi.org/10.1190/segam2015-5899618.1

EDITED REFERENCES

Note: This reference list is a copyedited version of the reference list submitted by the author. Reference lists for the 2015 SEG Technical Program Expanded Abstracts have been copyedited so that references provided with the online metadata for each paper will achieve a high degree of linking to cited sources that appear on the Web.

REFERENCES

Bale, R., Marchand, T., Wilkinson, K. and J. Deere, 2013, The design and application of converted-wave COVs: CSEG GeoConvention, Expanded Abstracts, 1–6.

Cary, P. W., 1999, Common-offset-vector gathers: an alternative to cross-spreads for wide-azimuth 3D surveys: 69th Annual International Conference and Exhibition, SEG, Expanded Abstracts, 1496–1499.

Gaiser, J. G., 2014, General definition of reflection-point coverage for P- and PS-wave COV data: 76th Annual International Conference and Exhibition, EAGE, Extended Abstracts, D202.

Stewart, R., and J. Gaiser, 2011, Application and interpretation of converted waves: SEG Continuing Education Course.

Vermeer, G. J. O., 1998, 3D symmetric sampling: Geophysics, **63**, 1629–1647. http://dx.doi.org/10.1190/1.1444459.

Vermeer, G.J.O., 2002, 3D seismic survey design: SEG.

DOI http://dx.doi.org/10.1190/segam2015-5899618.1